



Training and recovery behaviors of exchange bias in FeNi/Cu/Co/FeMn spin valves at high field sweep rates

D.Z. Yang^{a,b}, A. Kapelrud^a, M. Saxegaard^a, E. Wahlström^{a,*}

^a Institutt for fysikk, NTNU, NO-7491 Trondheim, Norway

^b The Key Laboratory for Magnetism and Magnetic Materials of Ministry of Education, Lanzhou University, Lanzhou 730000, China

ARTICLE INFO

Article history:

Received 1 September 2011

Received in revised form

20 April 2012

Available online 15 May 2012

Keywords:

Antiferromagnet

Exchange bias

Training effect

ABSTRACT

Training and recovery of exchange bias in FeNi/Cu/Co/FeMn spin valves have been studied by magnetoresistance curves with field sweep rates from 1000 to 4800 Oe/s. It is found that training and recovery of exchange field are proportional to the logarithm of the training cycles and recovery time, respectively. These behaviors are explained within the model based on thermal activation. For the field sweep rates of 1000, 2000 and 4000 Oe/s, the relaxation time of antiferromagnet spins are 61.4, 27.6, and 11.5 in the unit of ms, respectively, much shorter than the long relaxation time ($\sim 10^2$ s) in conventional magnetometry measurements.

© 2012 Elsevier B.V. All rights reserved.

1. Introduction

The exchange bias (EB) effect in ferromagnetic/antiferromagnetic systems has been intensely studied in the last decade because of their physical complexity and important applications [1,2]. The technological importance lies in the pinning effect of the antiferromagnet (AFM) layers in which the hysteresis loop of the ferromagnet (FM) can be shifted away from the origin point by the amount of the exchange field (H_E), and is usually accompanied with an enhanced coercivity (H_C). Changes of H_E and H_C are accordingly directly related to the spin configuration of the AFM layer through the exchange coupling [3]. Among the variety of effects related to the EB phenomenon, the training effect is an important effect that reflects the AFM spin dynamic process during repeated hysteresis loops. It is ascribed to that the spin structure of the AFM layer deviates from its equilibrium configuration and approaches another equilibrium triggered by subsequent reversals of the FM magnetization. Nowadays, studies of AFM spin dynamic behaviors with training effect in both experiments and theories have been widely reported [4–13]. Because most of studies are limited to long timescales (> 1 s), by the usually quite long measurement time in magnetometry approaches, the relaxation time of AFM spin are usually reported in second timescale ($\sim 10^2 - 10^4$ s) [4–6]. In contrast, at shorter measurement timescales the relaxation time of exchange bias system was demonstrated to cover a wide range ($\sim 10^{-8} - 10^{11}$ s)

[15–18], which has been ascribed to the magnetization reversal mechanism of FM layer [14]. Hence, the report *only* on AFM spin dynamic behavior in the millisecond timescale is still sparse. In addition, recently attempt frequencies up to 10^{12} Hz in AFM layer have been reported [19], which indicated a much shorter relaxation timescale of AFM spin than earlier anticipated. Therefore, it is necessary and interesting to study the AFM spin dynamic process at short timescale (technologic importance < 1 s).

In this paper, we have studied the EB training and recovery behaviors at the *millisecond timescale* based on the electrical transport measurements in FeNi/Cu/Co/FeMn spin valves. The experiments show that at high field sweep rates recovery time of exchange field after training procedures is three orders of magnitude shorter than the values observed by usual magnetometry techniques, and the relaxation of magnetoresistance (MR) is demonstrated in the millisecond timescale. These clearly indicate that AFM spin dynamic behaviors can be studied and resolved down to the millisecond timescale utilizing the ordinary resistance measurements.

2. Experiment and results

The spin valves of Si (001)/Cu (10 nm)/Fe₂₀Ni₈₀ (3 nm)/Cu (3 nm)/Co (3 nm)/FeMn (8 nm)/Ta (3 nm) were prepared by a magnetron sputtering system. The base pressure was 2×10^{-5} Pa and the Ar pressure was 0.3 Pa during the deposition. The 10 nm Cu buffer layer was used to stimulate the fcc (1 1 1) preferred growth of the FeMn layer in order to enhance the EB. A magnetic field of 130 Oe was applied in the film plane during deposition to induce the uniaxial anisotropy and thus the EB.

* Corresponding author at: Institutt for fysikk, NTNU, NO-7491 Trondheim, Norway.

E-mail address: erik.wahlstrom@ntnu.no (E. Wahlström).

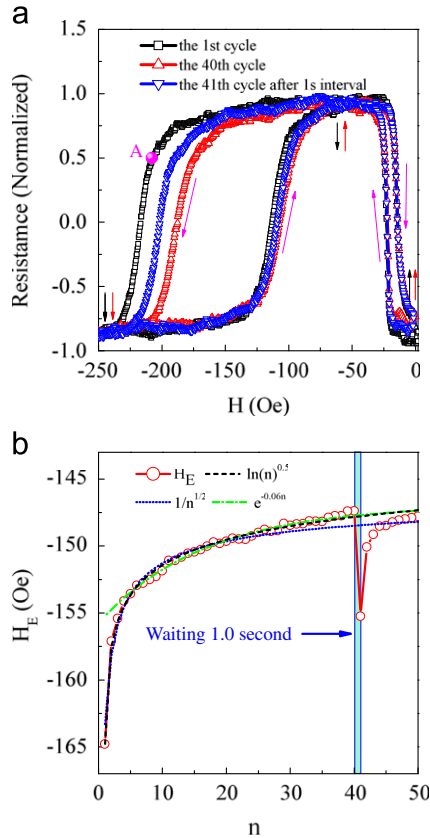


Fig. 1. (a) The magnetoresistance curves used to map the training effect for FeNi/Cu/Co/FeMn spin valve at the first, 40th and 41st (after 1 s waiting time) cycles with the field sweep rate of 4000 Oe/s. The resistance is dependent on corresponding magnetization configurations of FeNi (black left arrow) and Co (red right arrow). (b) The exchange field H_E as a function of the number of cycles n . The blue dot, green dash dot and black dash lines are the fitted data with the $1/\sqrt{n}$, $e^{-0.06n}$ and $\ln(n)$, respectively. (For interpretation of the references to color in this figure caption, the reader is referred to the web version of this article.)

Magnetoresistance (MR) measurements were performed to probe the switching behaviors of the pinned layer for different subsequent hysteresis loops. The magnetic field was provided by home-built Helmholtz coils, and MR was measured in real-time system with 2 M/s sampling rate. To study training and recovery of the EB, we first performed 40 consecutive MR measurements with a fixed field sweep rate to characterize the training procedures. Then we stopped the magnetic field sweep with an waiting time t . Finally 10 consecutive MR measurements with the same field sweep rate were measured in order to observe and confirm the EB recovery. For each sweep rate, t varied from 0.1 to 10 s.

The spin valves and MR curves of the training and recovery effects at the 1st, 40th and 41st cycles with the field sweep rate of 4000 Oe/s are displayed in Fig. 1(a). At large negative field the Co and FeNi magnetizations are parallel and pointing down. When the field is increased above the switch field of the Co layer, about -110 Oe, the Co magnetization reverses and resistance switches from low value (-1) to high value ($+1$). When the field is further increased above the switch field of the FeNi layer, about -15 Oe, its magnetization reverses, the two magnetizations become parallel once more but this time pointing up, and resistance switches to low value (-1). If the field is then decreased, the two magnetizations will remain parallel until the negative switch field of the FeNi layer is reached at -25 Oe, when its magnetization reverses and resistance switches to high value. When the field is further reduced and reverses the Co magnetization, the two magnetizations align in parallel, and resistance changes to its

low value. For all MR curves the hysteresis loops of the Co layer are shifted and fully separated from the hysteresis loops of FeNi layer due to the FeMn pinning effect, therefore the MR curves directly reflect the switching behaviors of the Co and the FeNi layers in detail [20]. Comparing the hysteresis loops of the Co layer in the first, and 40th MR curves, the switching field of the descent branch shifts more sharply than that of the ascent one, demonstrating the asymmetric magnetization reversal. However, after the magnetic field sweep is stopped for 1 s, a recovery is observed in the 41st MR curve. It contrasts to the behavior in the case of normally low field sweep rate, in which substantial recovery was only observed after several hours of waiting time [4]. The H_E is plotted as a function of cycles n in Fig. 1(b). The H_E gradually decreases with the cycle n , has an obvious resilience after 1 s waiting time and finally decreases. For the training procedure, the H_E versus n is fitted by a linear functions of $1/\sqrt{n}$, $e^{-0.06n}$ and $\ln(n)$. It is found that the logarithm function yields the best fit, except for initial point $n=1$ [8,10].

To further study the recovery of the trained EB, we measured the recovery rate R as a function of t at different field sweep rates, where $R = [H_E(41) - H_E(40)] / [H_E(1) - H_E(40)] \times 100(\%)$. Fig. 2(a) shows the dependence of R on t at different field sweep rates. The R increases with the increasing t as a linear function of $\log(t)$.

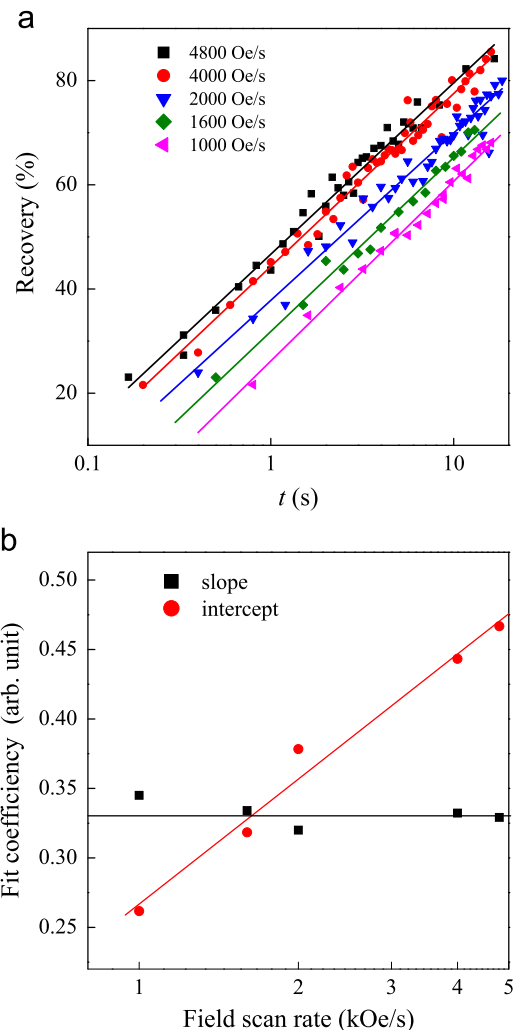


Fig. 2. (a) The recovery of H_E as a function of the waiting time t with different sweep rates. The solid lines display the linear fits of the $\ln(t)$. (b) The slope and the offset values as a function of the field sweep rate. The solid lines are the linear fits of the logarithm of the field sweep rate.

More remarkably, for a fixed waiting time t , R correspondingly increases with the increasing field sweep rate. This logarithm behavior is in a good agreement with the previous experiments in NiFe/FeMn system, while the recovery rate is several orders of magnitude faster than the value in the low field sweep rate case [4]. The slope and the intercept as a function of the field sweep rate are shown in Fig. 2(b). The slope displays little change with different field sweep rates whereas the intercept increases greatly as the field sweep rate increases in approximate linear function of the logarithm of the field sweep rate.

To investigate the dynamic behavior of the EB with high resolution, we observed the evolution of MR after setting the magnetic field from the positive saturation field to -210 Oe (the point A in Fig. 1(a)) near the switch field. As shown in Fig. 3, MR initially decreases sharply and then gradually reaches a constant. The small fluctuations in the curves are caused by 50 Hz AC noise in the amplifying circuit. Remarkably, a crossover of the normalized MR from positive to negative has been observed, demonstrating the reversal of the magnetization of the Co layer. It is possible to link the time dependence of MR with the magnetic viscosity in the Co/FeMn bilayers [7], in which the magnetization of the pinned layer gradually reverses due to the thermally activated process in Co/FeMn bilayers. Because the reversal process in the EB at the first cycle consists in the single domain wall motion [6], the change of MR here is proportional to the amounts of the reversal magnetization in the pinned layer. Shown

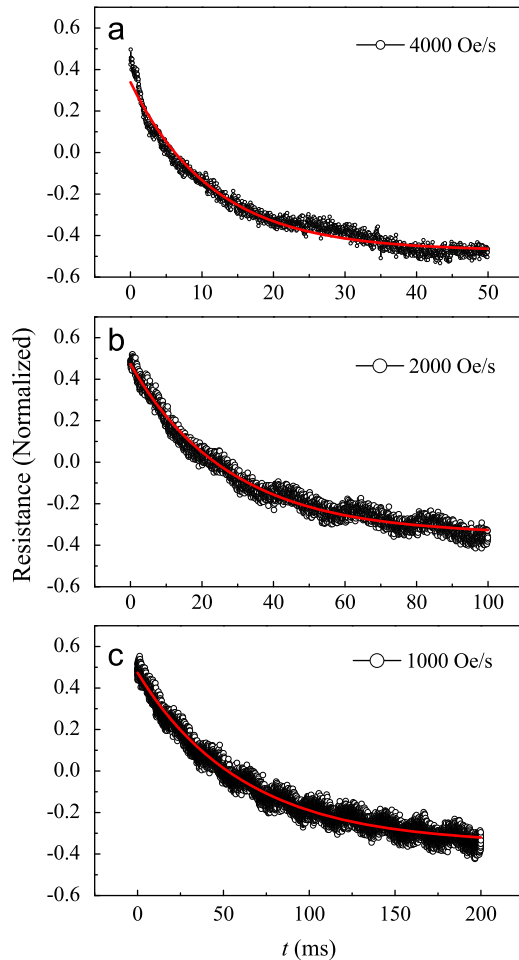


Fig. 3. The time dependence of the resistance after the external magnetic field is swept to -210 Oe (point A in Fig. 1(a)) from positive saturation field with different field sweep rates (a) 4000 Oe/s, (b) 2000 Oe/s, and (c) 1000 Oe/s. The solid lines are fits to the first-order exponential decay.

as the solid line in Fig. 3, the evolutions of MR are described well by a first order exponential decay. From fitting the data, we extracted the relaxation times τ which are 11.5, 27.6, and 61.4 ms for the field sweep rate at 4000, 2000 and 1000 Oe/s, respectively. This is again in contrast to the long relaxation time (~ 800 s) in the conventional approaches [6]. One can also note that the relaxation time decreases with the increasing field sweep rate.

3. Discussion

The above results show that the recovery and relaxation of the EB at high field sweep rates are faster than that earlier observed [4–7]. Below we will interpret the experimental results in conventional models for AFM and training effects.

Firstly we consider the change and magnitude of the relaxation time constants at different field sweep rates shown in Fig. 3. The time constant for the relaxation can be described by an ordinary Arrhenius law $\tau = \nu_{\sigma}^{-1} \exp(E_{\sigma}/k_B T)$, where ν_{σ} is the attempting frequency and $E_{\sigma} = KV$ represents the AFM energy barrier, K is the AFM anisotropy and V is the AFM grain volume. According to the AFM grain volumes distribution, we can divide the E_{σ} into three different categories [10]: (i) small E_{σ} (small grain size), which follows the FM magnetization at the timescale of the experiment. (ii) Medium energy E_{σ} (medium grain size) which will determine the EB dynamics at the timescale we investigate. (iii) Large E_{σ} (large grain size), which is a stable configuration over the timescale of the experiment. Assuming a typical uniaxial anisotropy constant of 1×10^6 erg/cm³ and ν_{σ} to be 1×10^9 Hz, then the average grain size of category (ii) is correspondingly about 9 nm extension, based on the relaxation time in Fig. 3. Accordingly, the relaxation time decreasing with the increasing field sweep rate demonstrates an apparent increase in attempt frequency ν_{σ} .

The EB recovery and relaxation at high field sweep rates can still be explained well with the model based on thermal activation [4,23]. As shown in Fig. 2(a), the logarithm time recovery relationship indicates a thermally activated reversal process involving the AFM spin configuration. To explain our data, the activation energy spectrum model simply based on a two-level system is adopted [23,24]. In our case the two level system represents an individual AFM grain or domain switching from a positive to a negative exchange energy with respect to the FM layer. For the system with a wide energy barrier distribution, ΔH_E can be expressed in terms of the AFM activation energy spectrum $q(E)$: $\Delta H_E = q(E)k_B T \ln(\nu_{\sigma} t)$, which is taken from Eq. (1) in Ref. [4]. According to the equation, the slope observed for all field rates in Fig. 2(b) is a constant due to the same $q(E)$, while the intercept variation is mainly due to the different activated AFM energy ranges and the time delay at the different field sweep rates.

Finally, for the training process H_E is proportional to $\ln(n)$ at high field sweep rates in Fig. 1(b), which can be compared to the usual power law ($1/\sqrt{n}$) and the exponential (e^{-2n}) relationships. We model this through following Binek et al. [21,22]. At beginning, the equilibrium AFM interface magnetization is defined $S_{AFM}^c = \lim_{n \rightarrow \infty} S_{AFM}(n)$. Each positive and negative deviation $\delta S_n = S_{AFM}(n) - S_{AFM}^c$ of the AFM interface magnetization from its equilibrium value will increase the total free energy F of the system by ΔF . The relaxation of the system towards equilibrium is determined by the Landau–Khalatnikov (LK) equation [25]: $\zeta \dot{S}_{AFM} = -\partial \Delta F / \partial S_{AFM}$, where ζ is a phenomenological damping constant and ΔF is the function of δS . In Binek's model under the assumption $\Delta F(\delta S) = \Delta F(-\delta S)$, a series expansion of ΔF up to the fourth order in δS yields $\Delta F = \frac{1}{2} a(\delta S)^2 + \frac{1}{4} b(\delta S)^4 + O(\delta S)^6$. Evaluating the free energy expression with a leading term of second

and fourth order in δS will result in the $e^{-\alpha n}$ [22] and $1/\sqrt{n}$ [21] evolution, respectively.

However, our understanding of the system is that we have a nonvanishing odd order term. This is an effect of working at a time scale where we also have substantial coupling at the FM/AFM interface due to large grains that are too large to follow the oscillating exchange coupling of the FM. Instead that portion of the ensemble of grain will orient itself gradually according to the mean coupling induced by the FM in a monotonic fashion. Accordingly we also have to consider the expansion of ΔF from first order of δS . We then assume $\delta S: \Delta F = f(n)(\delta S)^1 + O(\delta S)^2$, where the $f(n)$ indicates that the change in the AFM interface magnetization and δS_n is dependent on the training procedures n . By replacing \dot{S} with $[S(n+1)-S(n)]/\lambda$, with λ being the relevant experimental time constant and the free energy expression of the first order into the LK equation, we obtain an implicit sequence equation: $\zeta'(S(n+1)-S(n)) = -f(n)$, where $\zeta' = \zeta/\lambda$. The sum over N cycles of this equation with variable n yields $H_E(N+1) \propto S(N+1) = S(1) - \sum_{n=1}^N f(n)/\zeta'$.

Since we do not know the exact energy distribution $F(V)$ of our system, we make a first-order approximation assuming a constant distribution of AFM grain volumes. An estimate of the change in thermally activated part of the interface magnetization can be found through: $f(n) = \int_{V_n}^{V_{n+1}} F(V) dV$, using a thermally activated grain volume V_n which is found through the Arrhenius expression and a constant distribution in volume $F(V)$ we find that $f(n)$ will follow a $\ln(n+1) - \ln(n)$ dependence, a logarithmic dependence of the exchange bias. This approximation may only be valid at large n when the overall reorientation due to the changed mean field dominate over other training effects. We also note that the training process H_E is proportional to $\ln(n)$ has also been reported at low field sweep rates [8], where the training speed is several orders of magnitude slower than the values reported here.

In summary, for the AFM spins the relaxation time in the millisecond timescale is demonstrated when the bilayers are exposed to high field sweep rates. This behavior can be well explained in terms of a time constrained thermal activation. Our finding gives a new insight into the dynamic behavior of the AFM spins.

Acknowledgments

We gratefully acknowledge helpful and fruitful discussions with S.M. Zhou. The work was supported by the Norwegian Research

Council, Frinat project 171332. The author D.Z. Yang acknowledges the funding supported by the National Natural Science Foundation of China under Grand no. 11104122; the Fundamental Research Funds for the Central Universities lzujbky-2011-51.

References

- [1] J. Nogues, I.K. Schuller, Journal of Magnetism and Magnetic Materials 192 (1999) 203.
- [2] A.E. Berkowitz, K. Takano, Journal of Magnetism and Magnetic Materials 200 (1999) 552.
- [3] X.P. Qiu, D.Z. Yang, S.M. Zhou, R. Chantrell, K. O'Grady, U. Nowak, J. Du, X.J. Bai, L. Sun, Physics Review Letters 101 (2008) 147207.
- [4] J. Dho, C.W. Leung, M.G. Blamire, Journal of Applied Physics 99 (2006) 033910.
- [5] P.A.A. van der Heijden, T.F.M.M. Maas, W.J.M. de Jonge, J.C.S. Kools, F. Roozeboom, P.J. van der Zaag, Applied Physics Letters 72 (1998) 492.
- [6] E. Pina, C. Prados, A. Hernando, Physical Review B 69 (2004) 052402.
- [7] C. Leighton, I.K. Schuller, Physical Review B 63 (2001) 174419.
- [8] C.Y. Hung, M. Mao, S. Funada, T. Schneider, L. Miloslavsky, M. Miller, C. Qian, H.C. Hong, Journal of Applied Physics 87 (2000) 4915.
- [9] M.J. Carey, N. Smith, B.A. Gurney, J.R. Childress, T. Lin, Journal of Applied Physics 89 (2001) 6579.
- [10] M.K. Chan, J.S. Parker, P.A. Crowell, C. Leighton, Physical Review B 77 (2008) 014420.
- [11] T. Hughes, K. O'Grady, H. Laidler, R.W. Chantrell, Journal of Magnetism and Magnetic Materials 235 (2001) 329.
- [12] H.W. Xi, S. Franzen, S.N. Mao, R.M. White, Physical Review B 75 (2007) 014434.
- [13] A.G. Biternas, R.W. Chantrell, U. Nowak, Physical Review B 82 (2010) 134426.
- [14] B. Raquet, M.D. Ortega, M. Goiran, A.R. Fert, J.P. Redoules, R. Mamy, J.C. Ousset, A. Sdaq, A. Khmou, Journal of Magnetism and Magnetic Materials 150 (1995) L5.
- [15] F. Garcia, J. Moritz, F. Ernult, S. Auffret, B. Rodmacq, B. Dieny, J. Camarero, Y. Pennec, S. Pizzini, J. Vogel, IEEE Transactions on Magnetics 38 (2002) 2730.
- [16] J. Camarero, Y. Pennec, J. Vogel, M. Bonfim, S. Pizzini, M. Cartier, F. Ernult, F. Fetta, B. Dieny, Physical Review B 64 (2001) 172402.
- [17] A. M Goodman, K. O'Grady, H. Laidler, N.W. Owen, X. Portier, A.K. Petford-Long, F. Cebollada, IEEE Transactions on Magnetics 37 (2001) 565.
- [18] S. Sahoo, S. Plisetty, Ch. Binek, A. Berger, Journal of Applied Physics 101 (2007) 053902.
- [19] G. Valledo-Fernandez, N.P. Aley, J.N. Chapman, K. O'Grady, Applied Physics Letters 97 (2010) 222505.
- [20] J. Ventura, J.P. Araujo, J.B. Sousa, A. Veloso, P.P. Freitas, Physical Review B 77 (2008) 184404.
- [21] Ch. Binek, Physical Review B 70 (2004) 014421.
- [22] Ch. Binek, S. Plisetty, X. He, A. Berger, Physics Review Letters 96 (2006) 067201.
- [23] E. Fulcomer, S.H. Charap, Journal of Applied Physics 43 (1972) 4190.
- [24] M.R.J. Gibbs, J.E. Evetts, J.A. Leake, Journal of Materials Science 18 (1983) 278.
- [25] G. Vzdrik, S. Ducharme, V.M. Fridkin, G. Yudin, Physical Review B 68 (2003) 094113.